

Alterations in Pulmonary Ultrastructure and Morphometric Parameters Induced by Parainfluenza (Sendai) Virus in Rats During Postnatal Growth

WILLIAM L. CASTLEMAN, DVM, PhD

From the Department of Pathology, College of Veterinary Medicine, Cornell University, Ithaca, New York

The ultrastructural and morphometric effects of viral respiratory disease during postnatal lung growth were examined in weanling (22-day-old) and suckling (5-day-old) rats infected with parainfluenza Type 1 (Sendai) virus. Viral nucleocapsids and budding virions were identified by transmission electron microscopy in ciliated cells, mucous cells, and nonciliated bronchiolar epithelial cells of weanling rats at 5 days after inoculation and were associated with epithelial necrosis and erosion as well as hyperplasia of nonciliated bronchiolar epithelial cells. Interstitial pneumonia characterized in early stages by swelling and sloughing of Type 1 and Type 2 alveolar epithelial cells was also present at 5 and 7 days after inoculation. Lesions persisting at 30, 60, and 90 days after inoculation included multi-

focal connective tissue polyps in terminal bronchioles that partially obstructed bronchiolar lumens. Specific lung volume was greater ($P < 0.01$) in weanling rats at 30 and 60 days following viral infection than in control rats, and specific alveolar surface area was 42% greater ($P < 0.01$) in infected rats at 60 days after inoculation. Suckling rats infected during a phase of rapid postnatal lung growth at 5 days of age had 33% greater ($P < 0.02$) specific alveolar surface area and 48% greater ($P < 0.001$) mean terminal bronchiolar cross-sectional area when compared with control rats at 22 days of age. The results indicate that viral pulmonary infection during early life can induce acute and persistent alterations in pulmonary structure that could adversely affect lung function. (Am J Pathol 1984, 114:322-335)

VIRAL RESPIRATORY INFECTION during early life can result in severe acute disease that is characterized physiologically by increased airway resistance and morphologically by bronchiolitis with airway obstruction and interstitial pneumonia.¹⁻³ Children under 2 years of age are most susceptible to virus-induced pulmonary disease.¹ Retrospective and prospective studies suggest that virus-induced lung damage during infancy can result in persistent alterations in lung function and structure and could predispose individuals to obstructive lung disease in later life.^{1,4-6} The relatively higher risk of severe acute disease and subsequent pathologic sequelae associated with viral infection during infancy as compared with later life could be related to factors such as immature immunologic and nonimmunologic pulmonary defense mechanisms, age-associated susceptibility of cells in the lower respiratory tract to virus-initiated injury, and anatomic and physiologic features of young, growing lungs.^{1,7} Two structural features of importance in the lungs of infants are that they have

relatively small airways that may be predisposed to obstruction by inflammatory cell exudate and bronchiolar constriction and that they are undergoing the most accelerated phase of postnatal lung growth and development in the first 2 years of life and may be more susceptible to virus-induced dysplasia or hypoplasia than older, more fully developed lungs.^{1,8,9}

Viruses of major importance in causing bronchiolitis and pneumonia in infancy are respiratory syncytial virus, parainfluenza virus Types 1 and 3, and adenoviruses.^{1,10} Many virus-host model systems have been developed for studying virologic and immunologic aspects of viral infection of the lower respiratory tract.¹¹⁻¹⁴ The usefulness of these models in examining the potential effects of viral infection during early

Accepted for publication September 14, 1983.

Address reprint requests to Dr. William L. Castleman, Department of Pathology, College of Veterinary Medicine, Cornell University, Ithaca, NY 14853.

life on pulmonary structure and function and on postnatal lung growth have not been examined in detail. Because relatively little information on normal postnatal lung growth is available for species such as the cotton rat and the hamster, as compared with other rodents, and because only very mild bronchiolitis and pneumonia are induced in the model systems using ferrets and cotton rats infected with respiratory syncytial virus as compared with lesions described in infants,^{1,2} it is possible that these model systems will be of limited value.

A goal of this research was to examine the suitability of parainfluenza Type 1 (Sendai) virus infection in rats as a model of viral infection during early life. This is a spontaneous parainfluenza virus infection in a species for which there is abundant information available on postnatal lung growth.¹⁵⁻¹⁹ Three phases of postnatal lung growth are recognized in the rat: an early expansion phase (1-4 days of age); a tissue proliferation phase (4-13 days of age); and a later equilibrated growth phase (3 weeks to adult age).¹⁵⁻¹⁷ It is unclear whether all three phases exist in the postnatal development of human lungs. Histologic lesions induced by Sendai virus in rats have been described in detail.^{18,19} Little information is available on the cells in the rat lung susceptible to Sendai viral infection or on the ultrastructural alterations associated with cell infection. The specific objectives of this report are 1) to describe the ultrastructural lesions induced by Sendai virus in intrapulmonary airways and alveolar parenchyma of weanling rats and 2) to characterize quantitative alterations in lung morphometric parameters induced by Sendai virus in suckling rats (5 days of age) when they are in the tissue proliferation phase of lung growth and in weanling rats (22 days of age) when they are in the equilibrated phase of lung growth.

Materials and Methods

Animals and Virology

Outbred rats, Crl:CD(SD)BR (Charles River Breeding Laboratories, Inc., Portage, Michigan) were used in these studies. In the first experiment, weanling male rats 22 days old were purchased, screened for microbial pathogens, and housed as previously described.¹⁹ In the second experiment, pregnant female rats were purchased and housed under similar conditions. When the litters were 5 days old, they were assigned into control or infected groups. Litters in the two groups were identical in size, and individual suckling rats were closely comparable in weight. Pups were

maintained with their dams throughout the course of the experiment and were allowed to suckle.

Methods of viral propagation, inoculation, viral isolation, viral serology, and bacteriology have been described in detail.¹⁹ In summary, parainfluenza Type 1 (Sendai) virus was obtained from Dr. John C. Parker (Microbiological Associates, Inc., Walkersville, MD) and was propagated in 9-11-day-old embryonated chicken eggs. Infected weanling rats were inoculated intranasally following anesthesia with methoxyflurane with 0.05 ml of saline-diluted (1:10) allantoic fluid containing 10^2 TCID₅₀ (50% tissue culture infective dose) of Sendai virus. Control rats were anesthetized and received a similar intranasal volume of allantoic fluid from uninfected eggs. Suckling rats were inoculated in a similar manner, except that they were not anesthetized. Infected suckling rats received 0.025 ml of saline-diluted allantoic fluid containing 10^1 TCID₅₀ of virus at 5 days of age. Control suckling rats were given a similar volume of allantoic fluid from uninfected eggs. Lungs for viral isolation and sera were taken aseptically from 3 infected weanling rats at 1, 3, 5, 6, 7, 9, 12, 17, and 30 days after inoculation. The lungs were frozen in liquid nitrogen and stored at -65 C prior to attempted viral recovery. Viral isolation was attempted from the lungs of 3 control rats 6 days after inoculation with uninfected allantoic fluid, and the results were negative. For viral isolation and titration, serially 10-fold diluted lung homogenates (10% wt/vol) or allantoic fluid were inoculated onto BHK-21 cells grown in 24-well tissue culture plates. Endpoints for titration were determined using hemabsorption with chicken red blood cells. Titers were calculated by the method of Karber.²⁰

Light and Electron Microscopy

Weanling rats were killed by methoxyflurane anesthesia and exsanguination at 1, 2, 3, 5, 7, 9, 12, 17,

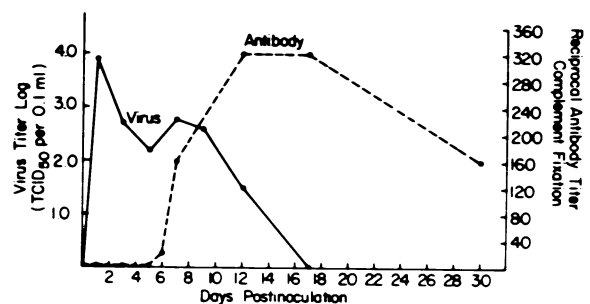


Figure 1—Lung viral and serum antibody titers from weanling rats infected with Sendai virus. Lung viral titers are expressed per 0.1 ml of 10% lung homogenate.

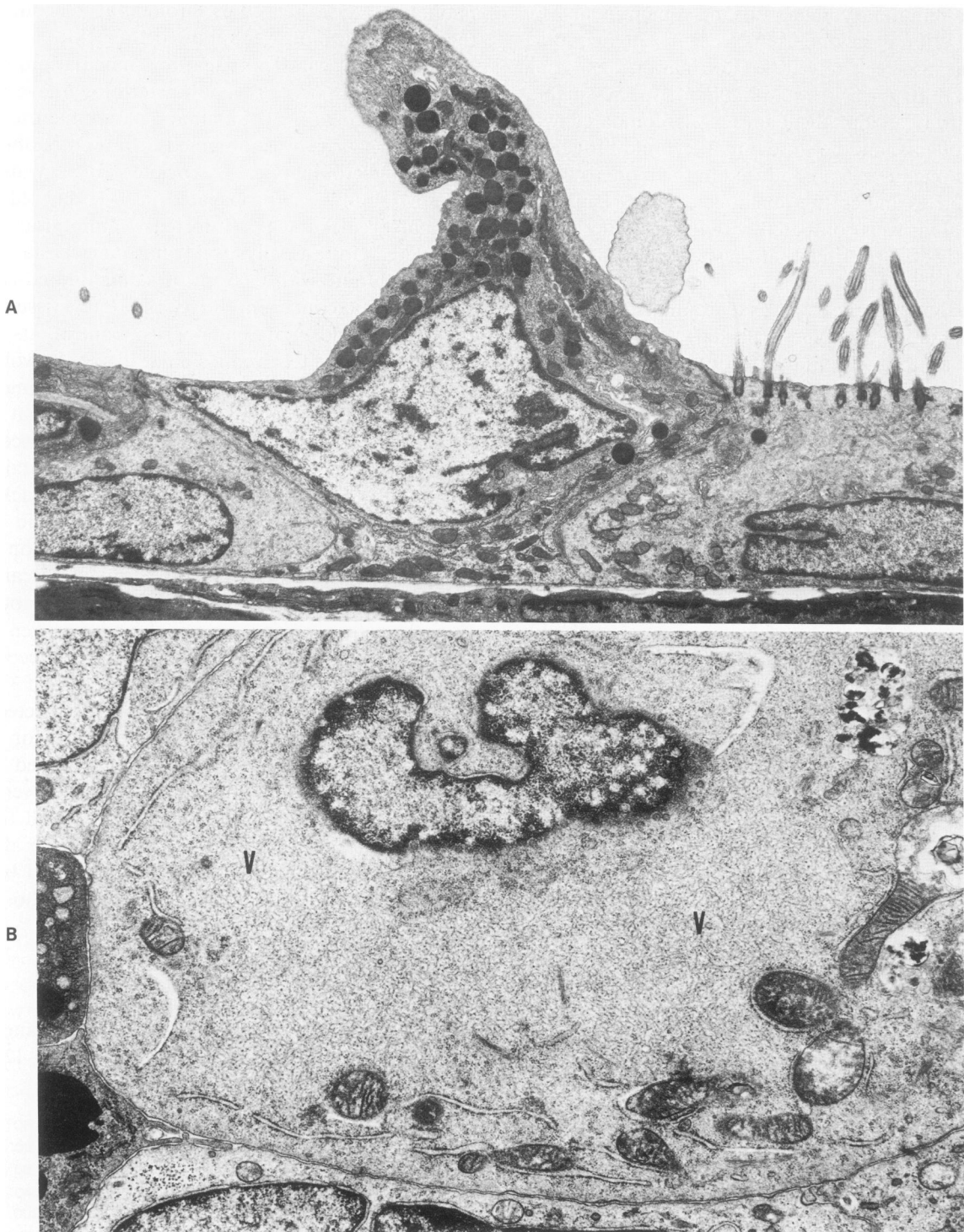


Figure 2A—Transmission electron micrograph. Nonciliated bronchiolar epithelial cell and ciliated cells from bronchiole of control rat. ($\times 6120$)
B—Nonciliated bronchiolar epithelial cell from a weanling rat at 5 days after inoculation. The cytoplasm is distended with aggregates of viral nucleocapsids (V). ($\times 14,970$)

30, 60, and 90 days after inoculation. Uninfected control groups were necropsied at 1, 7, 17, 30, 60, and 90 days after inoculation. At least 3 rats were in each group at periods of 1–12 days after inoculation. There

were at least 4 rats were in each group at 17, 30, 60, and 90 days after inoculation. Suckling rats were necropsied at 21 days of age. In both weanling and suckling rats, the lungs and trachea were excised and

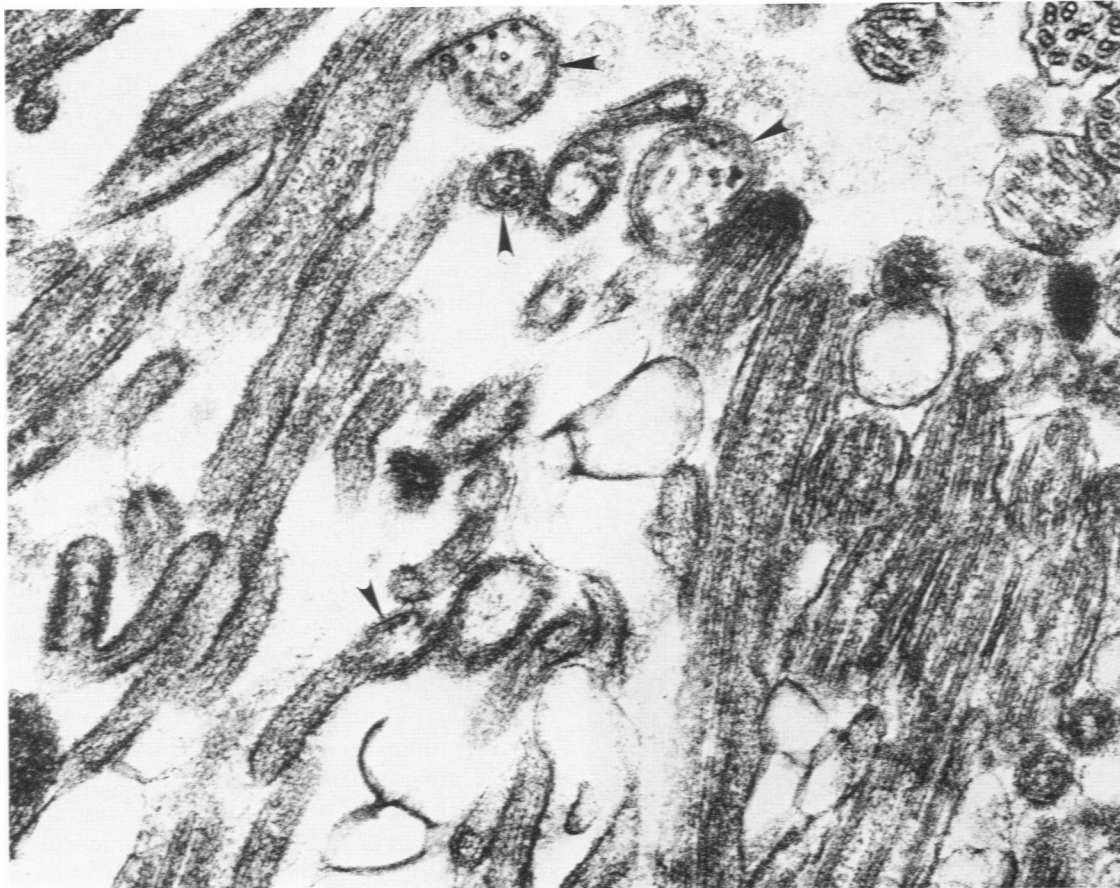


Figure 3—Transmission electron micrograph. Mature virions and budding virions (*arrowheads*) are associated with cilia and microvilli of a bronchiolar ciliated cell at 3 days after inoculation. Weanling rat. ($\times 51,075$)

fixed by tracheal perfusion at 30 cm of pressure with Karnovsky's fixative²¹ diluted 1:4.5 (550 milliosmolar) with 0.2 M cacodylate buffer. The lungs were dissected from the main stem bronchi, and lung volume was measured by fluid displacement.²² Serial transverse sections were taken of the left lungs and embedded in paraffin for preparation of hematoxylin and eosin (H&E)-stained sections. Sections were taken of the right cranial lung lobe for scanning and transmission electron microscopy as described.²³

Light-Microscopic Morphometry

Morphometric measurements were made on serial paraffin sections taken from the left lung of each animal. Measurements were based on 7–14 sections per lung. The number of sections examined varied with the size of the lung. Mean terminal bronchiolar cross-sectional area was calculated for each rat by photographing transverse sections of bronchioles by the use of defined criteria.²⁴ Photographs of bronchioles were measured with a digitizing tablet interfaced

with a microcomputer (Bioquant II, R and M Biometrics, Nashville, TN). Values for areas were not corrected for shrinkage associated with fixation and paraffin processing because accurate preprocessing measurement of bronchiolar area could not be made.

Volume densities of pulmonary parenchyma were measured as described^{25,26} with a 42-point, 21-line eyepiece graticule at an overall magnification of $\times 125$. Alveolar surface area was estimated by a light-microscopic method.²⁷ Measurements were made at a magnification of $\times 250$ on alveolar parenchymal fields selected by the use of a systematic sampling method from a random starting point.

Results

Studies of Weanling Rats Infected at 22 Days of Age

A summary of the virologic and viral serologic studies is presented in Figure 1. Virus could be recovered from lung homogenates of infected rats at time points between 1 and 12 days after inoculation.

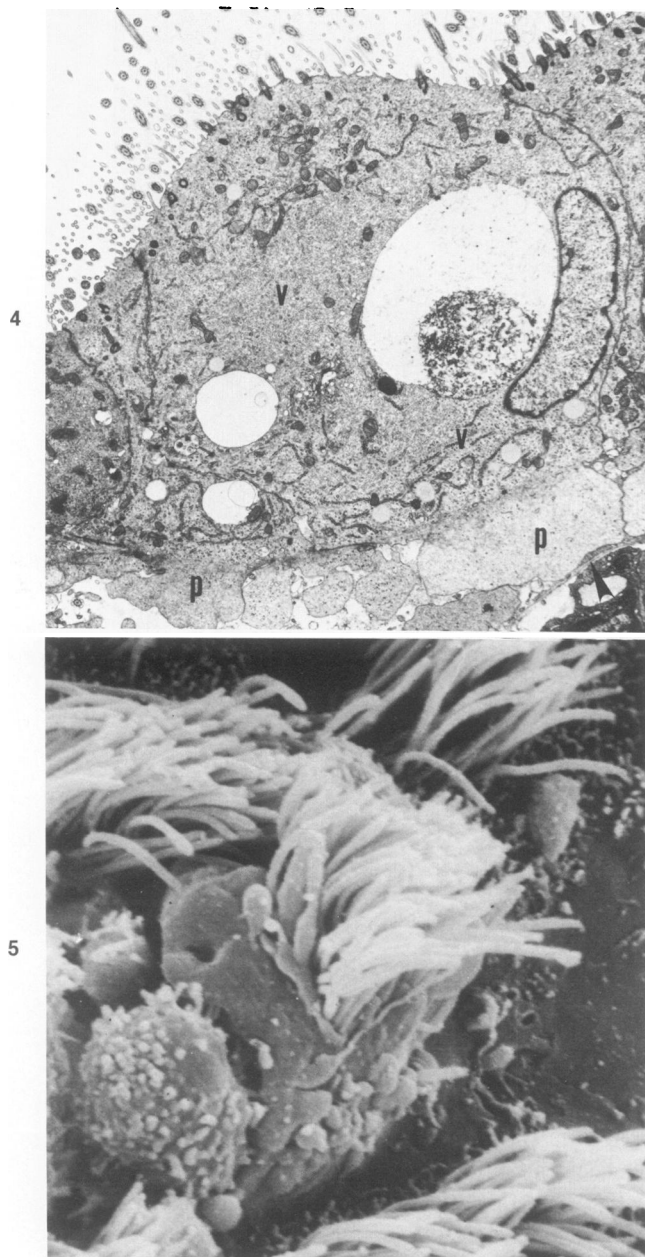


Figure 4—Transmission electron micrograph. Bronchiolar ciliated cell at 5 days. The cytoplasm contains aggregates of viral nucleocapsids (*v*) and vacuoles. The cell is separated from the subjacent basal lamina (*arrowhead*) and electron-lucent cell processes (*p*) extend from the basilar surface of the cell. Weanling rat. ($\times 4200$)
Figure 5—Scanning electron micrograph. Bronchiolar ciliated cell at 5 days. Cilia are clumped together and swollen. There are cytoplasmic protrusions on the lateral surfaces of the cell. Weanling rat. ($\times 8400$)

Complement-fixing antibody was first detected in serum at 6 days after inoculation. Neither virus nor antibody were detected in control rats.

Light and Electron Microscopy

Light-microscopic and ultrastructural lesions were not observed in lungs of infected rats until 3 days

after inoculation, and lesions were not observed in any control rats. The initial pulmonary alterations in infected rats occurred in bronchiolar epithelium. At 3 and 5 days after inoculation there was hypertrophy of ciliated and nonciliated bronchiolar epithelial cells. Viral nucleocapsids and budding virions were observed in these two cell types (Figures 2–4 and 7), and cytoplasmic accumulation of nucleocapsids appeared to account for cell hypertrophy in many of the cells. In ciliated cells, nucleocapsids were often positioned adjacent to membranes of cilia and microvilli, and maturing virions were budding from the surface of these cell processes (Figure 3). Morphologic evidence of cell damage in bronchiolar epithelium at 3, 5, and 7 days after inoculation included extension of cytoplasmic processes from basal and lateral cell surfaces (Figures 4 and 5), swelling of mitochondria and endoplasmic reticulum, with formation of large vacuoles (Figures 4–7), and cell necrosis and sloughing (Figures 5 and 6). In ciliated cells examined in rats at 5 days after inoculation, additional ultrastructural abnormalities included close interadherence or clumping of cilia, formation of compound cilia, internalization of ciliary axonemes, and formation of intracellular lumens (Figures 3 and 6). Multinucleated syncytial cells were occasionally present in bronchiolar epithelium. The densest inflammatory cell infiltrate in airways was noted at 5 days after inoculation and was predominantly composed of macrophages and neutrophils that were often closely associated with virus-infected cells (Figure 6). Neutrophils were rarely fused with ciliated cells containing aggregates of nucleocapsids (Figure 7). Macrophages in bronchiolar lumens occasionally contained virions and nucleocapsids in phagosomes.

At 5 days after inoculation there were large areas of bronchiolar epithelial hyperplasia (Figures 8 and 9). In many bronchioles the concurrent epithelial necrosis and sloughing and hyperplasia of epithelium with leukocytic infiltration resulted in complete obstruction of lumens. There were large areas of eroded bronchiolar mucosa at 7 days after inoculation. In other areas, low-cuboidal nonciliated cells in simple or stratified arrangement covered the bronchiolar surface. Mitotic figures were observed ultrastructurally in nonciliated bronchiolar epithelial cells at 3 and 5 days after inoculation. At 9 days after inoculation all bronchiolar mucosal surfaces were covered by cuboidal and columnar epithelial cells. At 7 and 9 days after inoculation, centrioles, fibrogranular aggregates, and basal bodies were observed in the apical cytoplasm of many of these cells, indicating ciliogenesis. Almost all bronchiolar epithelium appeared to be qualitatively normal by light- and electron-

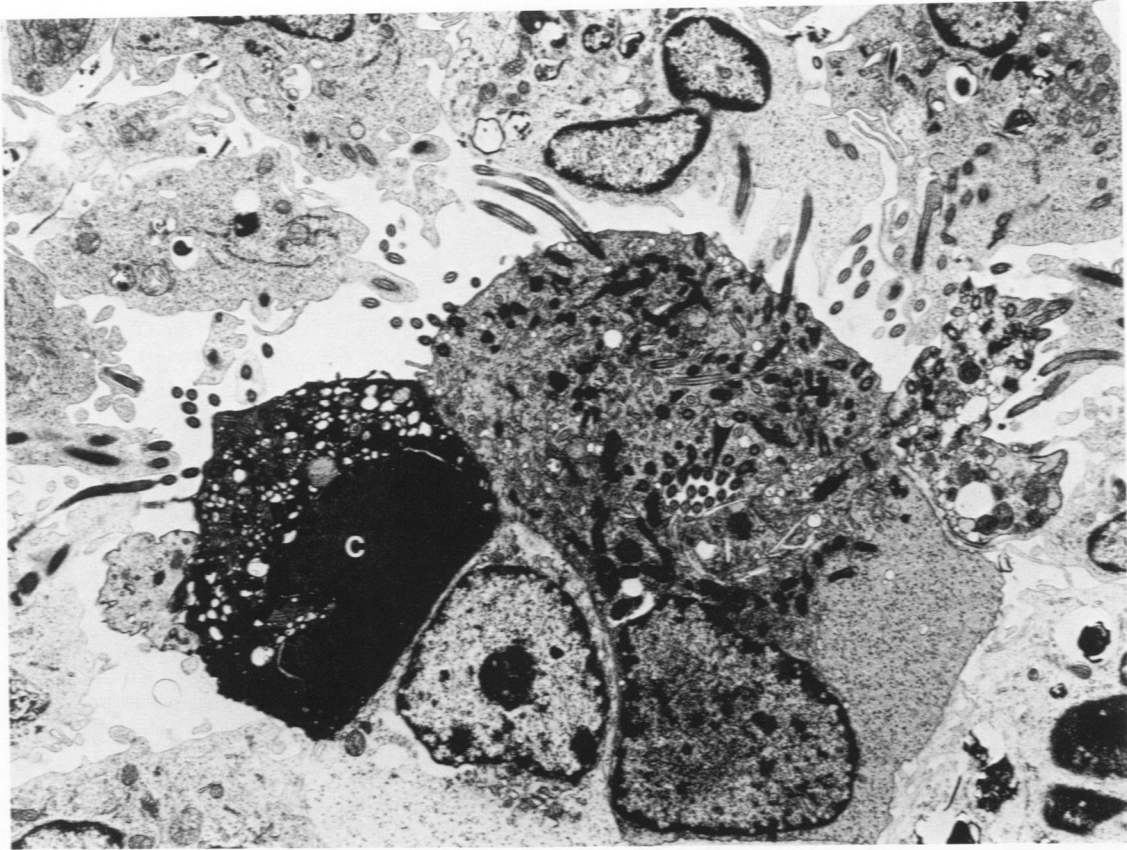


Figure 6—Transmission electron micrograph. Bronchiolar epithelium at 5 days after inoculation. A ciliated cell has an intracytoplasmic lumen with cilia (*arrowhead*) and axonemes that are internalized. An adjacent ciliated cell is necrotic (C). Macrophages in the lumen engulf cilia. Weanling rat. ($\times 5887$)

microscopic features by 17 days after inoculation. Occasional polyps of loose connective tissue and aggregates of macrophages persisted in bronchiolar lumens at this time.

Interstitial pneumonia was present in rats between 5 and 9 days after inoculation (Figure 10). The lesions were usually centered around bronchioles, although entire lobes were occasionally diffusely affected. At 5 days after inoculation, the mildest lesions observed were swelling of Type 1 alveolar epithelial cells with associated interstitial edema and septal aggregations of monocytes and macrophages (Figure 11). Intravascular aggregates of platelets were associated with endothelial cells that were separated from the adjacent external lamina (Figure 12). There was frequent swelling of endoplasmic reticulum and mitochondria in Type 2 alveolar epithelial cells, and these cells were partially separated from the adjacent basal lamina (Figures 13 and 14). Cytoplasmic processes of Type 2 alveolar epithelial cells were rarely partially engulfed by macrophages (Figure 13). Neither viral nucleocapsids nor budding virions were observed in the alveolar parenchyma by transmission electron microscopy. Bare basal laminae and alveolar deposits of serum

protein, fibrin, and neutrophils, and macrophages were present at 5 days after inoculation (Figures 10, 12, and 14). At 7 days after inoculation, alveolar aggregates of macrophages with a minimal number of interspersed neutrophils were located around terminal bronchioles. Interalveolar septa in the area were often thickened and edematous and contained many intra-septal macrophages and interstitial cells or fibroblasts (Figure 15). Septal epithelium included occasional multinucleated Type 2 alveolar epithelial cells (Figure 16). At 30, 60, and 90 days after inoculation, aggregates of macrophages, lymphocytes, and plasma cells were in peribronchiolar and perivascular areas. There was occasional partial luminal obstruction of terminal bronchioles and alveolar ducts by polyps of connective tissue associated with distortion and thickening of surrounding interalveolar septa (Figure 17).

Light-Microscopic Morphometry

Data on body weight and lung volume in weanling rats infected at 22 days of age is presented in Table 1 and Figure 18. There were no significant differences in lung volumes or body weights between infected and

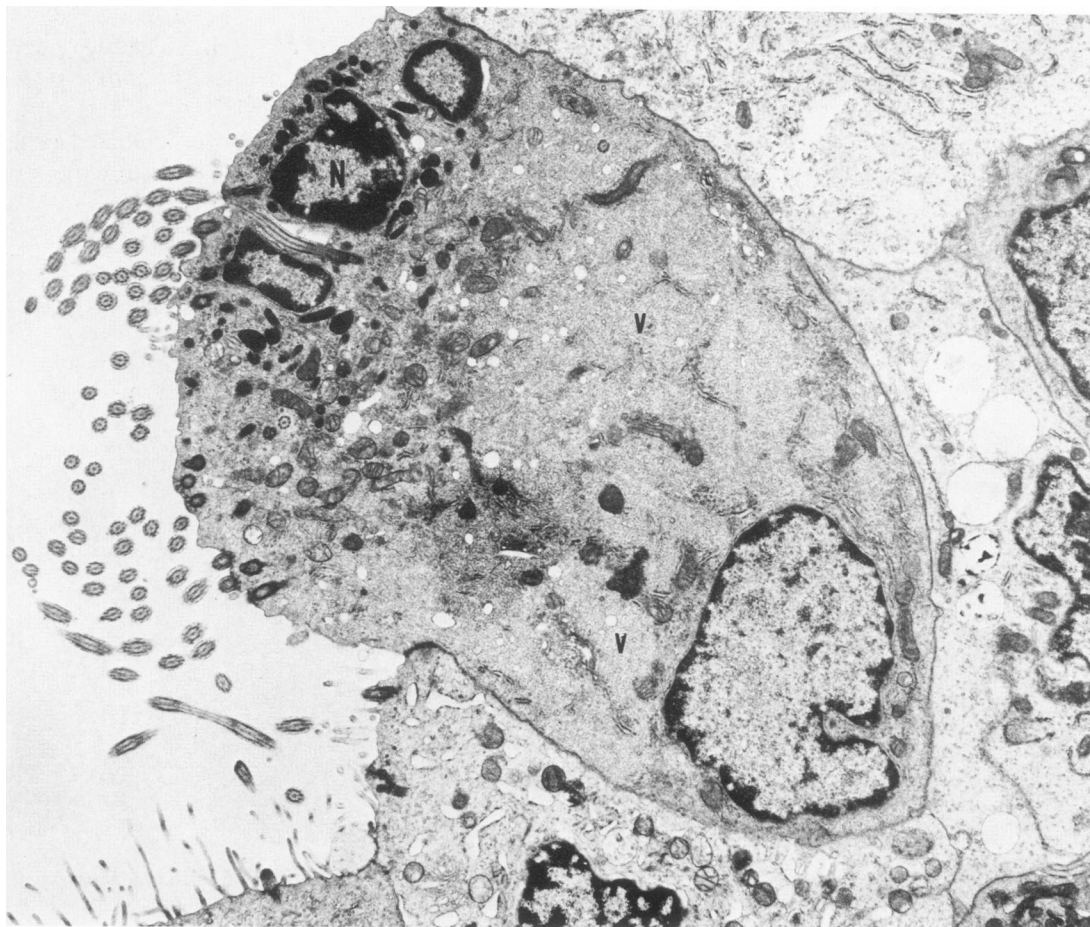


Figure 7—Transmission electron micrograph. A bronchiolar ciliated cell at 5 days after inoculation contains cytoplasmic accumulations of nucleocapsids (v), and a neutrophil (N) is fused with apical cytoplasm. Weanling rat. ($\times 7217$)

control rats at 7 and 17 days after inoculation. At 30 and 60 days after inoculation, lung volume and specific lung volume were significantly higher in infected rats, as compared with control rats. Specific lung volume in infected rats was 46% and 60% higher than in control animals at 30 and 60 days after inoculation, respectively. There were no significant differences in lung volume or specific lung volume at 90 days after inoculation. Because there were histologic lesions in terminal bronchioles and proximal acinar regions associated with significant lung volume changes in infected rats at 30 and 60 days after inoculation, more detailed morphometric evaluations of the lungs at these time points were deemed necessary. Values of terminal bronchiolar cross-sectional areas and alveolar surface areas on rats at 30 and 60 days after inoculation are presented in Table 2. Despite the presence of frequent focal obstructive nodules in terminal bronchioles of infected rats, there were no quantitatively demonstrable differences in terminal bronchio-

lar area between infected and control rats. Similarly, there were no significant differences in alveolar surface area between control and infected rats. At 60 days after inoculation, however, there was a 42% higher specific alveolar surface area in infected rats as compared with controls.

Studies on Suckling Rats Inoculated at 5 Days of Age

At 16 days after inoculation, all virus-inoculated rats had histologic lesions comparable in nature but more severe than those observed in weanling rats at 17 days after inoculation. The lesions in suckling rats were characterized by distortion of peribronchiolar tissue and interalveolar septa by connective tissue containing a low density of fibroblasts and collagen (Figure 19). There was occasional stenosis of terminal bronchiolar lumens and peribronchiolar and perivascular aggregates of macrophages, lymphocytes, and plasma cells.

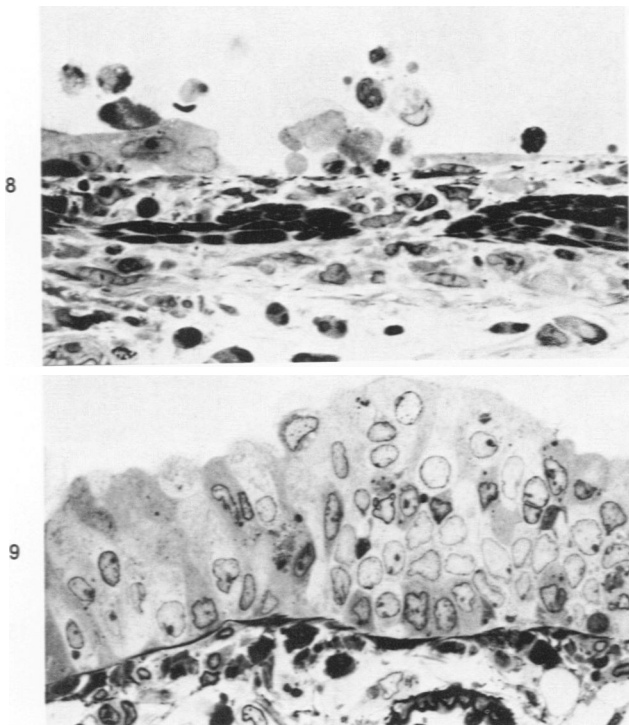


Figure 8—A bronchiole at 5 days after inoculation. There is sloughing of ciliated and nonciliated cells and erosion. Macrophages and neutrophils are in the bronchiolar lumen and wall and in peribronchiolar connective tissue. Weanling rat. (Epon-araldite section, methylene blue-azure II-basic fuchsin stain (EMAB), $\times 618$) **Figure 9**—Terminal bronchiole at 5 days after inoculation. There is marked hyperplasia of bronchiolar epithelium. Submucosa is edematous and contains macrophages, monocytes, and neutrophils. Weanling rat. (EMAB, $\times 586$)

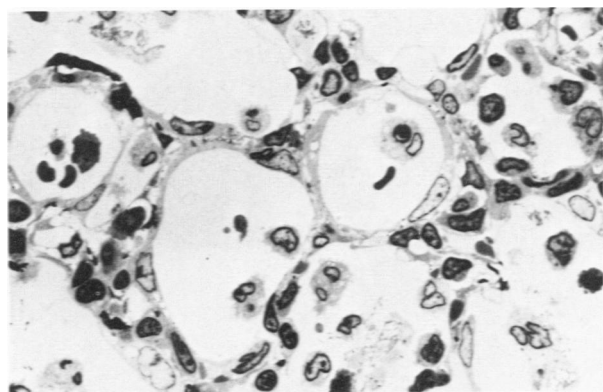
Morphometric parameters from virus-infected and control suckling rats are presented in Tables 3 and 4. Infected rats had lower brain and body weights than control rats, suggesting direct or indirect virus-induced suppression of somatic growth. Specific lung volume was greater in infected than in control rats, although there was no difference in absolute lung volume. There was an increase in the volume density of interstitial tissue in the virus-infected rats. Mean terminal bronchiolar cross-sectional area was 48% greater in infected than in control rats, and specific alveolar surface area was 33% higher in viral-infected animals. There was no difference in absolute alveolar surface area or other volume densities between infected and control rats.

Discussion

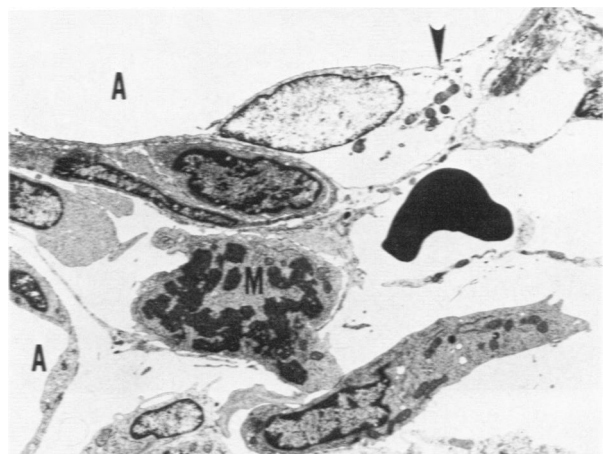
The results of this study demonstrate that Sendai virus infection in rats induces acute and persistent injury to intrapulmonary airways and alveolar paren-

chyma and that this damage is associated with alterations in pulmonary morphometric parameters.

In intrapulmonary airways, budding virions and cytoplasmic nucleocapsids were identified in ciliated, mucous, and nonciliated bronchiolar epithelial cells, suggesting that these cells can support viral replication and may be susceptible to direct virus-induced damage. These observations agree well with the findings for viral distribution in studies on Sendai viral infection in mice.²⁸⁻³⁰ The results from the virologic studies are comparable to those from studies in mice in that Sendai virus could be recovered from lung homogenates at times ranging from 1 to 12 days after inoculation.³⁰ As observed in other viral pathogenesis studies in the respiratory tract,^{11,12,30} productive viral infection was demonstrated by viral isolation procedures prior to the development of histologic or ultrastructural lesions. The recovery of virus prior to

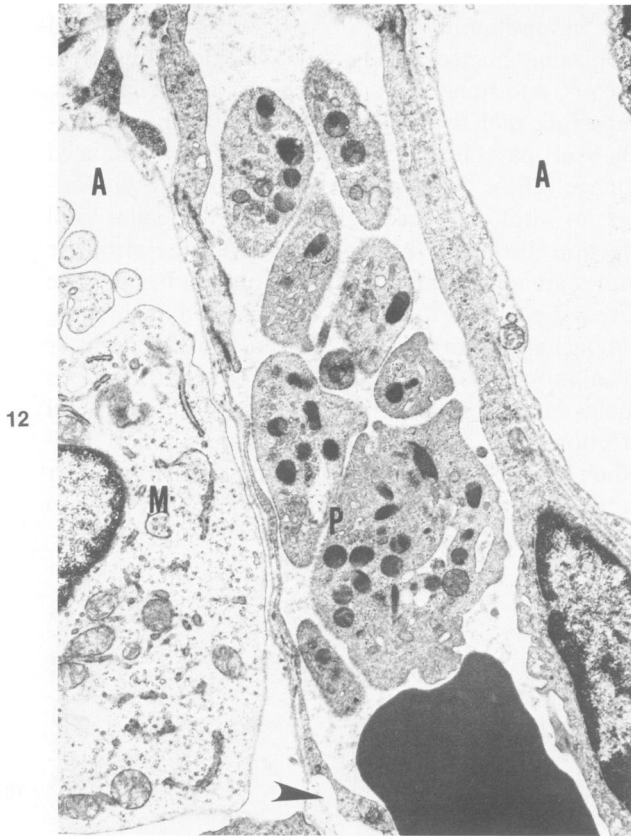


10



11

Figure 10—Alveolar parenchyma from a weanling rat at 5 days after inoculation. Interalveolar septa are thick and hypercellular and contain macrophages, other small mononuclear inflammatory cells, and neutrophils. Alveoli contain macrophages, cell debris, fibrin, and neutrophils. (EMAB, $\times 594$) **Figure 11**—Transmission electron micrograph. Interalveolar septum and alveolar spaces (A) at 5 days after inoculation. There is cytoplasmic swelling of a Type 1 alveolar epithelial cell (arrowhead) and edematous separation of septal elements. Macrophages, monocytes, and a free erythrocyte are in the septum, and a monocyte is in mitosis (M). Weanling rat. ($\times 2957$)

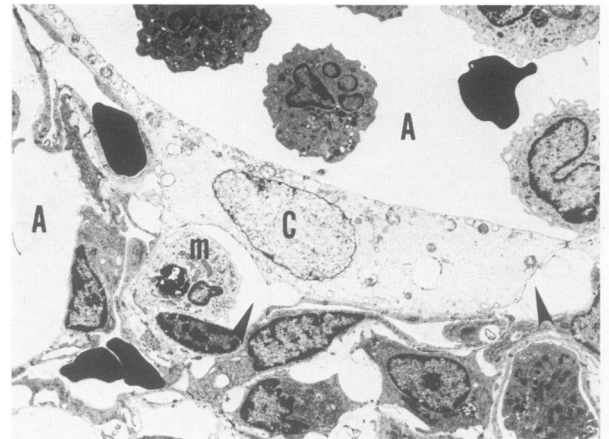


12

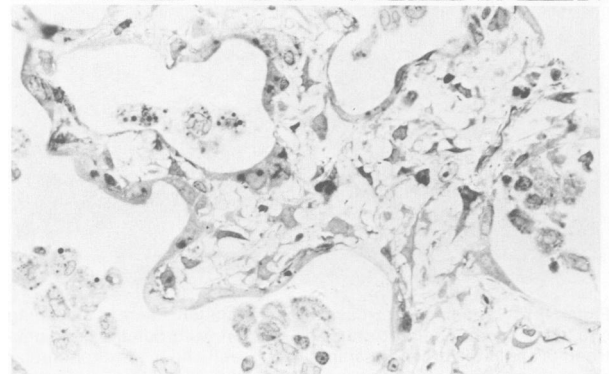


13

Figure 12—Transmission electron micrograph. Interalveolar septum and alveolar spaces (A) at 5 days after inoculation. There are aggregated platelets (P) in a capillary lumen. There are gaps between endothelial cytoplasm and the external lamina (arrowhead). A macrophage (M) is closely associated with a bare alveolar basement membrane. Weanling rat. (× 8661) **Figure 13**—Transmission electron micrograph. Type 2 alveolar epithelial cell at 5 days after inoculation. There is mitochondrial swelling (arrowheads), and an apical cytoplasmic protrusion (P) is partially engulfed by a macrophage. Weanling rat. (× 6558)



14



15

Figure 14—Transmission electron micrograph. Interalveolar septum and alveolar spaces (A) at 5 days after inoculation. A type 2 alveolar epithelial cell (C) is partially separated from the subjacent basal lamina (arrowheads). A macrophage (m) is interposed between the basal lamina and the type 2 cell. Macrophages and neutrophils are present in the septum and alveoli. Weanling rat. (× 2186) **Figure 15**—Alveolar parenchyma at 7 days after inoculation. Interalveolar septa are thick and contain many fusiform and stellate-shaped interstitial cells. Aggregates of macrophages are in alveoli. Weanling rat. (EMAB, × 480)

the observation of morphologic lesions is probably related to complete viral replication preceding any histologically detectable lesions such as cell necrosis as well as to the tissue sampling problems inherent in transmission electron microscopic studies. The virologic results in this study in rats differ from those in studies in mice in that peak viral titers in rat lung occurred at 1 day after inoculation, as compared with 3–9 days after inoculation for mice.^{29,30} It is possible that rats have neutralizing antibody in their lungs at an earlier postinoculation time than mice, thus inhibiting recovery of infectious virus at later times. Since the lungs were frozen prior to attempted viral isolation, however, it is also possible that viral preservation was poor in the lungs 1 day after inoculation due to nonspecific viral inhibitors associated with the inflammatory response that could have inactivated part of the viral activity prior to and after freezing and thawing.



16



17

Figure 16—Transmission electron micrograph. Multinucleated syncytial epithelial cell lining an interalveolar septum at 7 days after inoculation. Weanling rat. ($\times 4368$) **Figure 17**—Terminal bronchiole from a rat at 90 days. A polyp of connective tissue containing inflammatory cells protrudes into the bronchiolar lumen. Weanling rat. (H&E, $\times 98$)

The acute virus-induced airway epithelial damage included cell swelling, necrosis, syncytial epithelial cell formation, as well as ciliary abnormalities that would be expected to result in abnormalities in mucociliary clearance. There was an inflammatory cell infiltrate composed of neutrophils and macrophages in airways closely associated temporally with intraepithelial viral structures and detectable serum complement-fixing antibody. Much of the epithelial damage observed could have been mediated by inflammatory cell- or complement-dependent mechanisms.³⁰⁻³² The observation of neutrophil fusion with virus-infected ciliated cells is interesting because it suggests that intracellular as well as extracellular release of lyso-

somal enzymes and toxic oxygen metabolites could be mechanisms for neutrophil-mediated damage of viral-infected epithelial cells.^{31,32} Epithelial repair was rapid in airways and associated with epithelial hyperplasia and partial obstruction of bronchiolar lumens. Epithelial repair appeared to be accomplished through division of nonciliated bronchiolar epithelial cells and differentiation of nonciliated cells into ciliated cells, as has been demonstrated in studies on oxidant-induced bronchiolar injury.^{33,34} The partial obstruction of bronchiolar lumens by connective tissue polyps could be due to focal areas of delayed epithelial injury and organization of luminal exudate and/or focal induction of collagen synthesis and fibroblast proliferation by mediators released from inflammatory cells.³⁵

Acute cell injury in alveolar parenchyma included cytoplasmic swelling and detachment of Type 1 and Type 2 alveolar epithelial cells and minor alterations in capillary endothelial cells. The cell damage was not associated with viral structures that could be identified by electron microscopy. Studies in mice have demonstrated that Sendai virus can replicate in Type 2 alveolar epithelial cells, alveolar macrophages, and, in nude mice, Type 1 alveolar epithelial cells.^{28,29,30,36,37} Multinucleated syncytial Type 2 alveolar epithelial cells were observed in infected rats and were presumably a manifestation of viral infection through the activity of F glycoprotein of Sendai virus.³⁰ This cytopathic effect was not found in control rats. Although it is likely that at least some of the cell damage in interalveolar septa is mediated by direct virus-initiated injury, many of the alterations in epithelial and endothelial cells could be due to complement- and cell-mediated injury as part of a humoral or cellular immune response that has been demonstrated in Sendai virus infection³⁰ or due to neutrophil-mediated damage following the intraalveolar generation of chemotactic complement fragments such as C5a.^{31,38} The virus-initiated damage resulted in disorganization of alveolar parenchyma and fibrosis around terminal bronchioles and alveolar ducts.

The results indicate that viral infection in early postnatal life can affect airway and parenchymal development. Other studies have shown that pulmonary viral infection during prenatal lung development can induce pulmonary hypoplasia,³⁹ and adenoviral infection in infants has been associated with bronchiolitis obliterans and the unilateral hyperlucent lung syndrome, which is characterized in part by overinflation of alveolar parenchyma and hypoplasia of pulmonary arteries.¹ It was anticipated that Sendai viral infection in neonatal rats would suppress postnatal lung growth. The results suggest that the opposite may

Table 1 — Body Weights and Lung Volumes in Weanling Rats Infected with Sendai Virus

Days after inoculation (n)	Body weight (g)	Lung volume (cu cm)	Specific lung volume (cu cm/g)
7 days			
Control (8)	89.12 ± 3.38*	4.91 ± 0.20	5.52 ± 0.18
Infected (3)	79.83 ± 2.89	4.38 ± 0.65	5.46 ± 0.67
17 days			
Control (8)	146.15 ± 5.14	7.32 ± 0.24	5.02 ± 0.13
Infected (4)	137.20 ± 4.80	7.50 ± 0.34	5.51 ± 0.45
30 days			
Control (9)	242.60 ± 8.14	8.65 ± 0.49	3.55 ± 0.12
Infected (4)	214.49 ± 24.25	10.83 ± 0.15†	5.17 ± 0.54‡
60 days			
Control (4)	491.14 ± 5.91	11.75 ± 0.58	2.39 ± 0.12
Infected (4)	414.87 ± 11.83‡	15.76 ± 0.81‡	3.82 ± 0.24‡
90 days			
Control (4)	511.51 ± 13.34	15.05 ± 0.59	2.94 ± 0.07
Infected (4)	465.81 ± 26.74	15.67 ± 0.64	3.38 ± 0.17

* Mean ± SEM.

† Two-sided *t*-test, *P* < 0.05.‡ *P* < 0.01.

have occurred. Specific lung volume in infected rats was greater than that in controls several weeks after viral infection, and terminal bronchiolar cross-sectional area was increased in rats that had been infected at 5 days of age. In both suckling and weanling rats the increased specific lung volume was associated with an increase in specific alveolar surface area relative to that in control rats. There are several possible explanations for these increases in specific lung volume and specific alveolar surface area in the infected rats. First, viral bronchiolitis and pneumonia may have resulted in parenchymal and airway damage with subsequent decreases in alveolar septal and airway wall elasticity. This could result in greater lung expansion during fixation in infected rats and larger lung volumes and bronchiolar and alveolar surface areas. Second, the increase in specific lung volume could be largely due to indirect virus-induced suppression of body growth due to factors such as depressed appetite with a relative sparing effect of undernutrition on lung growth. Third, viral bronchiolitis and pneumonia may provide a direct or indirect stimulus for acceleration of postnatal pulmonary growth.

Virus-induced damage during postnatal growth of airways and alveoli could have altered the quantity and arrangement of collagen and elastin in these structures and reduced pulmonary elasticity. If this occurred, increased lung compliance could result in larger lung volumes at constant perfusion pressures in the infected rats. One would predict that the greater lung volumes would result from overexpansion of alveoli during fixation and that this enlargement would be manifested in the morphometric data.

There was no significant decrease in alveolar surface density (square centimeters of alveolar surface/cubic centimeters of lung volume) in either weanling or suckling rats that would be expected to occur if there were enlargement of alveoli resulting from decreased elasticity. It is unlikely that the 48% increase in specific alveolar surface area and the 31% increase in specific lung volume in viral infected suckling rats is solely the result of decreased lung elasticity, because there was no change in alveolar surface density. Since physiologic measurements of lung compliance were not measured, however, the possibility that alterations in lung volumes and areas are at least in part due to viral-induced changes in lung elasticity must be considered.

It is unlikely that the alterations in lung volume and alveolar surface area are the result of undernutri-

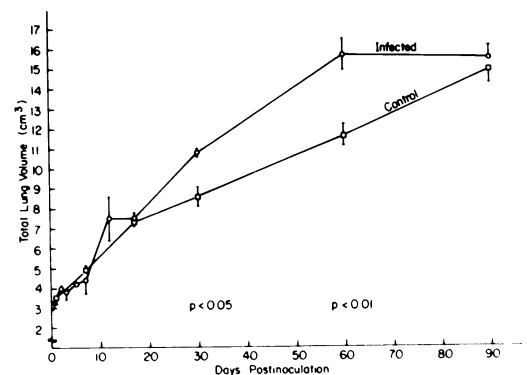


Figure 18 — Lung volume in infected and control weanling rats. Bar = SEM. Points at 30 and 60 days after inoculation are significantly different by two-sided *t*-test.

Table 2—Terminal Bronchiolar Area and Alveolar Surface Areas in Weanling Rats Infected With Sendai Virus

	30 days* Control	30 days* Infected	60 days* Control	60 days* Infected
Mean terminal bronchiolar cross-sectional area (sq $\mu \times 10^3$)	44.1 \pm 8.7 [†]	49.4 \pm 5.4	44.7 \pm 2.1	45.1 \pm 2.6
Alveolar surface density sq cm/cu cm	696.9 \pm 59.8	575.9 \pm 42.5	611.2 \pm 22.9	546.4 \pm 18.2
Alveolar surface area (sq cm)	5158.6 \pm 400.6	5302.3 \pm 411.9	6102.0 \pm 380.5	7290.6 \pm 206.4
Specific alveolar surface area (sq cm/g body weight)	19.2 \pm 1.4	25.1 \pm 2.3	12.4 \pm 0.7	17.6 \pm 0.8 [‡]

* After inoculation.

[†] Mean \pm 1 SE.[‡] $P < 0.01$, *t*-test.

tion resulting from altered milk or food intake in the virus-infected groups. There was no change in absolute lung volume or alveolar surface area in the virus-infected rats, whereas virus infection was associated with an absolute increase in terminal bronchiolar diameter in the virus-infected suckling rats. The disparity of results suggests a direct, although nonuniform, effect of viral infection on pulmonary morphometrics. Also, research on the effects of protein-deficient

diets on postnatal lung growth in hamsters indicates that protein restriction suppresses increases in body weight and lung volume with age, whereas it has little effect on airway diameter.⁴⁰

The interpretation that appears to be most consistent with the morphometric data is that Sendai virus infection at least transiently stimulated postnatal lung development and growth. Again, the possibility that decreased lung elasticity induced by Sendai virus during postnatal growth also contributed to the observed increase in lung volume cannot be completely excluded. Environmental stimuli such as hypoxia and cold have been clearly shown to accelerate postnatal increases in lung volume and alveolar surface area toward adult dimensions.^{41,42} The underlying mechanisms that are thought to be critical in this response, which is independent of changes in lung elasticity, are increased pulmonary blood flow or increased demand for oxygen.^{9,41,42} It could be that hypoxemia developing subsequent to virus-induced bronchiolitis and pneumonia was a stimulus for accelerated lung growth or that increased blood flow in the lung associated with inflammation acted as a stimulus.⁴² Alternatively, lung cell reparative proliferation following viral injury to bronchioles and alveolar parenchyma

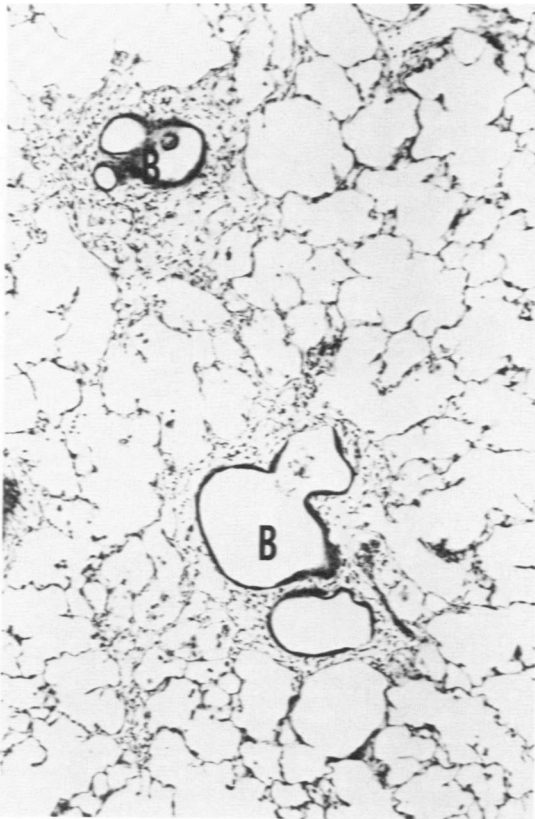


Figure 19—Terminal bronchioles and alveolar parenchyma from a suckling rat at 16 days after inoculation. There is distortion and thickening of alveolar septa and distortion and partial obstruction of terminal bronchioles (B) by loose connective tissue. (H&E, $\times 78$)

Table 3—Body Weights and Lung Volumes in Suckling Rats Infected With Sendai Virus

Parameters at necropsy	Control (n = 5)	Virus- infected (n = 5)
Body weight (g)	50.54 \pm 1.55*	35.74 \pm 1.27 [†]
Brain weight (g)	1.49 \pm 0.01	1.27 \pm 0.03 [†]
Lung volume (cu cm)	2.91 \pm 0.20	2.69 \pm 0.17
Specific lung volume (cu cm/100 g body weight)	5.75 \pm 0.27	7.54 \pm 0.14 [‡]

* Mean \pm SE.[†] Two-sided *t*-test, $P < 0.001$.[‡] $P < 0.02$.

Table 4—Light-Microscopic Morphometric Values in Suckling Rats Infected With Sendai Virus

	Control (n = 5)	Virus- infected (n = 5)
Volume density of alveolar parenchyma (Vvp)	0.863 ± 0.011*	0.842 ± 0.17
Volume density of airways (Vva)	0.080 ± 0.003	0.076 ± 0.009
Volume density of blood vessels (Vvv)	0.035 ± 0.007	0.028 ± 0.002
Volume density of interstitial tissue (Vvi)	0.020 ± 0.002	0.052 ± 0.007†
Alveolar surface density (Sva) (sq cm/cu cm)	452.84 ± 18.43	470.89 ± 13.80
Alveolar surface area (Sa) (sq cm ²)	1130.57 ± 59.17	1062.46 ± 64.43
Specific alveolar surface area (sq cm/g body weight)	22.39 ± 1.08	29.80 ± 1.80†
Mean terminal bronchiolar cross-sectional area (sq μ × 10 ³)	18.94 ± 1.56	28.09 ± 2.49‡

* Mean ± 1 SE.

† $P < 0.02$, *t*-test.‡ $P < 0.001$.

may have resulted in brief compensatory exaggeration of postnatal lung growth. Additional experiments will be required for the evaluation of the relative likelihood of these various possibilities and determination of whether the airway and alveolar lesions induced in weanling rats are reversible.

The effect of Sendai virus infection on morphometric parameters was more pronounced in the suckling rats that were infected at 5 days of age than in weanling rats infected at 22 days of age, and there was more severe histologic distortion of terminal bronchioles and associated alveolar parenchyma in the suckling rats. It is possible that the effect on suckling rats was more pronounced because the most rapid phase of alveolar growth and cell proliferation occurs in rats between 4 and 13 days of age,¹⁵⁻¹⁷ and it would be predicted that the most rapidly growing lung would be most susceptible to virus-induced alterations. Additional studies will be required to characterize the most important mechanisms in the pathogenesis of these alterations in pulmonary structure that may be influenced by age, including studies on pulmonary viral titer, systemic and pulmonary immune responses, and reparative responses of the growing lung to injury mediated by an intrapulmonary inflammatory response.

Human infants affected with viral lower respiratory tract disease develop erosive and necrotizing bronchiolitis with airway obstruction and interstitial pneumonia that is reported to result in acute and sometimes persistent increases in airway resistance and total lung volume.^{1,2,3,6} Animal models for investigation of detailed alterations in lung structure and function resulting from postnatal viral infection have been developed only to a minimal extent.¹¹⁻¹³ Sendai virus infection in suckling and weanling rats induces bronchiolitis and interstitial pneumonia that is of severity comparable to that described in infants with severe disease resulting from respiratory syncytial virus and other viral infections.^{1,2,19} Persistent obstructive polyps in terminal airways that could be associated with increased airway resistance and increases in specific lung volume and surface area result from Sendai virus infection in rats. Physiologic studies will be required for evaluation of the functional significance of these airway and parenchymal lesions. It is proposed that Sendai virus infection in weanling and suckling rats may be a useful experimental model in investigation of mechanisms important in the pathogenesis and therapeutic modulation of virus-induced lung damage during early life.

References

1. Wohl MEB, Chernick V: Bronchiolitis. *Am Rev Respir Dis* 1978, 118:759-781
2. Aherne W, Bird T, Court SDM, Gardner PS, McQuillin J: Pathological changes in virus infections of the lower respiratory tract in children. *J Clin Pathol* 1970, 23:7-18
3. Wohl MB, Stigol LC, Mead J: Resistance of the total respiratory system in healthy infants and infants with bronchiolitis. *Pediatrics* 1969, 43:495-509
4. Cumming GR, Macpherson RI, Chernick V: Unilateral hyperlucent lung syndrome in children. *J Pediatr* 1971, 78:250-260
5. Burrows B, Knudson R, Lebowitz M: The relationship of childhood respiratory illness to adult obstructive airway disease. *Am Rev Respir Dis* 1977, 115:751-760
6. Stokes GM, Milner AD, Hodges IGC, Groggins RC: Lung function abnormalities after acute bronchiolitis. *J Pediatr* 1981, 98:871-874
7. McIntosh K, Fishaut JM: Immunopathologic mechanisms in lower respiratory tract disease in infants due to respiratory syncytial virus. *Prog Med Virol* 1980, 26:94-118
8. Reid L: Influence of the pattern of structural growth of the lung on susceptibility to specific infectious diseases in infants and children. *Pediatr Res* 1977, 11:210-215
9. Inselman LS, Mellins RB: Growth and development of the lung. *J Pediatr* 1981, 98:1-15
10. Henderson FW, Clyde WA, Collier AM, Denny FW, Senior RJ, Sheaffer CI, Conley WG, Christian RM: The etiologic and epidemiologic spectrum of bronchiolitis in pediatric practice. *J Pediatr* 1979, 95:183-190
11. Prince GA, Jenson AB, Horswood RL, Camargo E, Chanock RM: The pathogenesis of respiratory syn-

- cytial virus infection in cotton rats. *Am J Pathol* 1978, 93:771-792
12. Prince GA, Porter, DD: The pathogenesis of respiratory syncytial virus infection in infant ferrets. *Am J Pathol* 1976, 82:339-352
 13. Collier AM, Clyde WA: Model systems for studying the pathogenesis of infections causing bronchiolitis in man. *Pediatr Res* 1977, 11:243-246
 14. Al-Darraj AM, Cutlip RC, Lehmkuhl HD, Graham DL: Experimental infection of lambs with bovine respiratory syncytial virus and *Pasteurella haemolytica*: Pathologic studies. *Am J Vet Res* 1982, 42:224-229
 15. Burri PH, Dbaly J, Weibel ER: The postnatal growth of the rat lung: I. Morphometry. *Anat Rec* 1974, 178: 711-730
 16. Burri PH: The postnatal growth of the rat lung: III. Morphology. *Anat Rec* 1974, 180:77-98
 17. Kauffman SL, Burri PH, Weibel ER: The postnatal growth of the rat lung: II. Autoradiography. *Anat Rec* 1974, 180:63-76
 18. Carthew P, Sparrow S: Sendai virus in nude and germ-free rats. *Res Vet Sci* 1980, 29:289-292
 19. Castleman WL: Respiratory tract lesions in weanling outbred rats infected with Sendai virus. *Am J Vet Res* 1983, 44:1024-1031
 20. Hawkes RA: General principles underlying laboratory diagnosis of viral infections, *Diagnostic Procedures for Viral, Rickettsial and Chlamydial Infections*. 5th edition. Edited by EH Lennette, NJ Schmidt. Washington, DC, American Public Health Association, 1979, pp 34-35
 21. Karnovsky MJ: A formaldehyde-glutaraldehyde fixative of high osmolality for use in electron microscopy (abstr). *J Cell Biol* 1965, 27:137a-138a
 22. Scherle W: A simple method for volumetry of organs in qualitative stereology. *Mikroskopie* 1970, 26:56-60
 23. Castleman WL, Dungworth DL, Schwartz LW, Tyler WS: Acute respiratory bronchiolitis: An ultrastructural and autoradiographic study of epithelial cell injury and renewal in rhesus monkeys exposed to ozone. *Am J Pathol* 1980, 98:811-840
 24. Matsuba K, Thurlbeck WM: The number and dimensions of small airways in nonemphysematous lungs. *Am Rev Respir Dis* 1971, 104:516-524
 25. Weibel ER: *Stereological Methods*. New York, Academic Press, 1979, pp 82-83
 26. Freere RH, Weibel ER: Stereologic techniques in microscopy. *J Roy Micros Soc* 1967, 87:25-34
 27. Weibel ER: A simplified morphometric method for estimating diffusing capacity in normal and emphysematous human lungs. *Am Rev Respir Dis* 1973, 107: 579-588
 28. Ward JM, Houchens DP, Collins MJ, Young DM, Reagan RL: Naturally-occurring Sendai virus infection of athymic nude mice. *Vet Pathol* 1976, 13:36-46
 29. Brownstein DG, Smith AL, Johnson EA: Sendai virus infection in genetically resistant and susceptible mice. *Am J Pathol* 1981, 105:156-163
 30. Parker JC, Richter CB: *Viral diseases of the respiratory system, The Mouse in Biomedical Research*. Edited by HL Foster, JD Small, JG Fox. New York, Academic Press, 1982, pp 110-134
 31. Fantone JC, Kunkel SL, Ward PA: Chemotactic mediators in neutrophil-dependent lung injury. *Ann Rev Physiol* 1982, 44:283-293
 32. Slauson DO: The mediation of pulmonary inflammatory injury. *Adv Vet Sci Comp Med* 1982, 26:99-153
 33. Evans MJ, Johnson LV, Stephens RJ, Freeman G: Renewal of the terminal bronchiolar epithelium in the rat following exposure to NO₂ or O₃. *Lab Invest* 1976, 35:246-257
 34. Lum H, Schwartz LW, Dungworth DL, Tyler WS: A comparative study of cell renewal after exposure to ozone or oxygen: Response of terminal bronchiolar epithelium in the rat. *Am Rev Respir Dis* 1978, 118: 335-345
 35. Bitterman PB, Rennard SI, Hunninghake GW, Crystal RG: Human alveolar macrophage growth factor for fibroblasts. Regulation and partial characterization. *J Clin Invest* 1982, 70:806-822
 36. Zurcher C, Burek JD, Van Nunen MCJ, Meihuizen SP: A naturally occurring epizootic caused by Sendai virus in breeding and aging rodent colonies: I. Infection in the mouse. *Lab Anim Sci* 1977, 27:955-962
 37. Mills J: Effects of Sendai virus infection on function of cultured mouse alveolar macrophages. *Am Rev Respir Dis* 1979, 120:1239-1244
 38. Shaw JO, Henson PM, Henson J, Webster RO: Lung inflammation induced by complement-derived chemotactic fragments in the alveolus. *Lab Invest* 1980, 42: 547-558
 39. Moe JB, Osburn BI, Schwartz LW, Anderson J, Johnson KP: Experimental adenovirus SV-40 pneumonia in fetal rhesus monkeys. Pathologic and virologic studies. *Lab Invest* 1979, 41:211-219
 40. Brody JS, Vaccaro C: Postnatal formation of alveoli: interstitial events and physiologic consequences. *Fed Proc* 1979, 38:215-223
 41. Lechner AJ, Banchemo N: Lung morphometry in guinea pigs acclimated to cold during growth. *J Appl Physiol* 1980, 48:886-891
 42. Lechner AJ, Banchemo N: Lung morphometry in guinea pigs acclimated to hypoxia during growth. *Respir Physiol* 1980, 42:155-169